Electron interactions in bilayer graphene: Marginal Fermi liquid and zero-bias anomaly

Electron interactions in bilayer graphene: Marginal Fermi liquid and zero-bias anomaly

Rahul Nandkishore and Leonid Levitov
Department of Physics, Massachusetts Institute of Technology, 77 Massachusetts Avenue, Cambridge, Massachusetts 02139, USA
(Received 6 June 2010; published 17 September 2010)

We analyze the many-body properties of bilayer graphene (BLG) at charge neutrality, governed by long-range interactions between electrons. Perturbation theory in a large number of flavors is used in which the interactions are described within a random phase approximation, taking account of dynamical screening effect. Crucially, the dynamically screened interaction retains some long-range character, resulting in $\log^2$ renormalization of key quantities. We carry out the perturbative renormalization group calculations to one loop order and find that BLG behaves to leading order as a marginal Fermi liquid. Interactions produce a log squared renormalization of the quasiparticle residue and the interaction vertex function while all other quantities renormalize only logarithmically. We solve the RG flow equations for the Green's function with logarithmic accuracy and find that the quasiparticle residue flows to zero under RG. At the same time, the gauge-invariant quantities, such as the compressibility, remain finite to $\log^2$ order, with subleading logarithmic corrections. The key experimental signature of this marginal Fermi liquid behavior is a strong suppression of the tunneling density of states, which manifests itself as a zero bias anomaly in tunneling experiments in a regime where the compressibility is essentially unchanged from the noninteracting value.

DOI: 10.1103/PhysRevB.82.115431 PACS number(s): 73.22.Pr

I. INTRODUCTION

Bilayer graphene (BLG), due to its unique electronic structure of a two-dimensional gapless semimetal with quadratic dispersion,[1] offers an entirely new setting for investigating many-body phenomena. In sharp contrast to single layer graphene, the density of states in BLG does not vanish at charge neutrality and thus even arbitrarily weak interactions can trigger phase transitions. Theory predicts instabilities to numerous strongly correlated gapped and gapless states in BLG.[2–6] These instabilities have been analyzed in models with unscreened long-range interactions,[2] dynamically screened long-range interactions,[3] and in models where the interactions are treated as short range.[4–6] Irrespective of whether one works with short-range interactions or with screened long-range interactions, the instability develops only logarithmically with the energy scale. However, dynamically screened Coulomb interactions have been shown to produce $\log^2$ renormalization of the self-energy[7] and vertex function.[3] Such strong renormalization can result in significant departures from noninteracting behavior on energy scales much greater than those characteristic for the onset of gapped states. However, there is as yet no systematic treatment of the $\log^2$ divergences. In this paper, we provide a systematic treatment of the effects of dynamically screened Coulomb interactions, focusing on the renormalization of the Green's function, and using the framework of the perturbative renormalization group (RG).

We analyze the RG flow perturbatively in the number of flavors, given by $N=4$ in BLG. We use perturbation theory developed about the noninteracting fixed point and calculate the renormalization of the fermion Green's function and of the Coulomb interactions. We demonstrate that the quasiparticle residue and the Coulomb vertex function undergo $\log^2$ renormalization while all other quantities renormalize only logarithmically. The quasiparticle residue and the Coulomb vertex function, moreover, are not independent but are related by a Ward identity which stems from gauge invariance symmetry. Therefore, at $\log^2$ order, BLG behaves as a marginal Fermi liquid.

We solve the RG flow equations with logarithmic accuracy, finding that the quasiparticle residue flows to zero under RG. This behavior manifests itself in a zero bias anomaly in the tunneling density of states (TDOS). We conclude by extracting the subleading (single log) renormalization of the electron mass, as a correction to the log square RG. This calculation allows us to predict the interaction renormalization of the electronic compressibility in BLG, a quantity which is interesting both because it is directly experimentally measurable and because it allows us to contrast the slow single log renormalization of the compressibility with the fast $\log^2$ renormalization of the TDOS.

The structure of the perturbative RG for BLG has strong similarities to the perturbative RG treatment of the one dimensional Luttinger liquids.[4,8–10] We recall that in the Luttinger liquids, the Green's function acquires an anomalous scaling dimension, which manifests itself in a power law behavior of a quasiparticle residue that vanishes on shell. In addition, the electronic compressibility in the Luttinger liquids remains finite even as the quasiparticle residue flows to zero. Finally, in the Luttinger liquids, there are logarithmic divergences in Feynman diagrams describing scattering in the particle-particle and particle-hole channels, corresponding to mean-field instabilities to both Cooper pairing and charge density wave ordering. However, when both instabilities are taken into account simultaneously within the framework of the RG, they cancel each other out, so that there is no instability to any long-range ordered phase at low energies.[8]

Exactly the same behavior follows from our RG analysis of BLG, including the cancellation of the vertices responsible for the pairing and charge density ordering. However, the diagrams in this instance are $\log^2$ divergent and even after the leading $\log^2$ divergences are canceled out, there remains a subleading single log instability. Nevertheless, this

single log instability manifests itself on much lower energy scales than the $\log^2$ RG flow. Therefore, over a large range of energies, bilayer graphene can be viewed as a two dimensional analog of the one-dimensional Luttinger liquids.

Our treatment of the $\log^2$ renormalization in BLG is somewhat reminiscent of the situation arising in two-dimensional disordered metals.[11] In the latter, the $\log^2$ divergences of the Green's function and of the vertex function stem from the properties of dynamically screened Coulomb interactions, which exhibit "unscreening" for the transferred frequencies and momenta such that ω/q^2 is large compared to the diffusion coefficient. Furthermore, the divergent corrections to the Fermi-liquid parameters, as well as conductivity, compressibility and other two-particle quantities in these systems, are only logarithmic. This allows to describe the RG flow of the Green function due to the $\log^2$ divergences by a single RG equation[12] of the form

$$\partial G/\partial \xi = -\frac{\xi}{4\pi^2 g} G,$$

where g is the dimensionless conductance. The suppression of the quasiparticle residue, described by this equation, manifests itself in a zero-bias anomaly in the tunneling density of states, readily observable by transport measurements.

II. DYNAMICALLY SCREENED INTERACTION

We begin by reviewing some basic facts about BLG. BLG consists of two AB stacked graphene sheets (Bernal stacking). The low-energy Hamiltonian can be described in a "two-band" approximation, neglecting the higher bands that are separated from the Dirac point by an energy gap $W \sim 0.4$ eV.[1] There is fourfold spin/valley degeneracy. The wave function of the low-energy electron states resides on the A sublattice of one layer and B sublattice of the other layer. The noninteracting spectrum consists of quadratically dispersing quasiparticle bands $E_{\pm} = \pm p^2/2m$ with band mass $m \approx 0.054 m_e$. We work throughout at charge neutrality, when the Fermi surface consists of Fermi points. The discrete pointlike nature of the Fermi surface is responsible for most of the similarities to the Luttinger liquids.

Although the canonical Hamiltonian has opposite chirality in the two valleys, a suitable unitary transformation on the spin-valley-sublatttice space brings the Hamiltonian to a form where there are four flavors of fermions, each governed by the same 2×2 quadratic Dirac-type Hamiltonian.[13] We introduce the Pauli matrices that act on the sublattice space τ_i, and define $\tau_{\pm} = \tau_1 \pm i\tau_2$, and $p_{\pm} = p_x \pm i p_y$, and hence write[14]

$$H = H_0 + \frac{e^2}{2\kappa} \sum_{\mathrm{x,x'}} \frac{n(\mathbf{x}) n(\mathbf{x}')}{|\mathbf{x}-\mathbf{x}'|}, \tag{1}$$

$$H_0 = \sum_{\mathbf{p},\sigma} \psi^{\dagger}_{\mathbf{p},\sigma} \left(\frac{p_+^2}{2m}\tau_+ + \frac{p_-^2}{2m}\tau_- \right) \psi_{\mathbf{p},\sigma}. \tag{2}$$

Here $\sigma = 1,2,3,4$ is a flavour index, $n(\mathbf{x}) = \Sigma_\sigma n_\sigma(\mathbf{x})$ is the electron density, summed over spins, valleys and sublattices while the dielectric constant κ incorporates the effect of polarization of the substrate. Note that the single-particle Hamiltonian H_0 takes the same form for each of the four fermion flavors and is thus $SU(4)$ invariant under unitary rotations in the flavor space.

The Coulomb interaction sets a characteristic length scale and a characteristic energy scale (Bohr radius and Rydberg energy)[3]

$$a_0 = \frac{\hbar^2 \kappa}{me^2} \approx 10\kappa \ \text{Å}, \quad E_0 = \frac{e^2}{\kappa a_0} \approx \frac{1.47}{\kappa^2} \ \text{eV}. \tag{3}$$

In Eq. (1), we have approximated by assuming that the interlayer and intralayer interaction are equal. This approximation may be justified by noting that the interlayer spacing $d \approx 3$ Å is much less than the characteristic length scale a_0, Eq. (3). Within this approximation, Hamiltonian (1) is invariant under $SU(4)$ flavor rotations.[13]

We note that for $\kappa \sim 1$ the energy E_0 value is comparable to the energy gap parameter $W \sim 0.4$ eV of the higher BLG bands (see Ref. 15 for a discussion of four band model of BLG). This suggests that there is some interaction induced mixing with the higher bands of BLG. However, since a four-band analysis is exceedingly tedious, here we focus on the weak coupling limit $E_0 \ll W$, where the two-band approximation, Eq. (1), is rigorously accurate. We perform all our calculations in this weak coupling regime and then extrapolate the result to $E_0 \approx 1.47 \ \text{eV}\kappa^{-2}$. Since the low energy properties should be independent of the higher bands, we believe this approximation correctly captures, at least qualitatively, the essential physics in BLG. Meanwhile since W is the maximum energy scale up to which the two-band Hamiltonian, Eq. (1), is valid, we use W as the initial ultraviolet (UV) cutoff for our RG analysis.

We wish to obtain a RG flow for the problem (1) by systematically integrating out the high-energy modes. However, the implementation of this strategy is complicated by the long-range nature of the unscreened Coulomb interaction. Within perturbation theory, the long-range interaction gives contributions which are relevant at tree level, making it difficult to come up with a meaningful perturbative RG scheme. Therefore, it is technically convenient to perform a two-step calculation, where we first take into account screening within the random-phase approximation (RPA) and then carry out an RG calculation with the RPA screened effective interaction. We emphasize that it is necessary to consider the full *dynamic* RPA screening of the Coulomb interaction since a static screening approximation does not capture the effects we discuss below.

The dynamically screened interaction may be calculated by summing over the RPA series of bubble diagrams, to obtain a screened interaction. The RPA approach to screening may be justified by invoking the large number $N=4$ of fermion species in BLG. The screened interaction takes the form

$$U(\omega,\mathbf{q}) = \frac{2\pi e^2}{\kappa|\mathbf{q}| - 2\pi e^2 \Pi(\omega,\mathbf{q})}. \tag{4}$$

Here $\Pi(\omega,\mathbf{q})$ is the noninteracting polarization function, which can be evaluated analytically.[3,16] Here we will need an

expression for $\Pi(\omega,\mathbf{q})$ in terms of Matsubara frequencies ω, derived in Ref. 3, where it was shown that the quantity $\Pi(\omega,\mathbf{q})$ depends on a single parameter $2m\omega/q^2$, and is well described by the approximate form

$$\Pi(\omega,\mathbf{q}) = -\frac{Nm}{2\pi}\frac{\ln 4\ \dfrac{\mathbf{q}^2}{2m}}{\sqrt{\left(\dfrac{\mathbf{q}^2}{2m}\right)^2 + u\omega^2}}, \quad u = \frac{4\ln^2 4}{\pi^2}, \tag{5}$$

where $N=4$ is the number of fermion species. The dependence [Eq. (5)] reproduces $\Pi(\omega,\mathbf{q})$ exactly in the limits $\omega \ll \mathbf{q}^2/2m$ and $\omega \gg \mathbf{q}^2/2m$, and interpolates accurately in between. We discover upon substituting Eq. (5) in Eq. (4) that the dynamically screened interaction is retarded in time but crucially is only marginal at tree level. It therefore becomes possible to develop the RG analysis perturbatively in weak coupling strength, by taking the limit of $N \gg 1$.

Since the quantity $\Pi(\omega,\mathbf{q})$ vanishes when $q \to 0$, the RPA screened interaction [Eq. (4)] retains some long-range character, exhibiting unscreening for $\omega \gg \mathbf{q}^2/2m$. This will lead to divergences in Feynman diagrams of a $\log^2$ character.

III. SETTING UP THE RG

To calculate the RG flow of the Hamiltonian, Eq. (1), in the weak coupling regime, we begin by writing the zero-temperature partition function Φ as an imaginary-time functional field integral. We have

$$\Phi = \int D\psi^\dagger D\psi \exp(-S_0[\psi^\dagger,\psi] - S_1[\psi^\dagger,\psi]), \tag{6}$$

$$S_0 = \sum_\sigma \int \frac{d\omega d^2p}{(2\pi)^3}\psi^\dagger_{\sigma,\omega,\mathbf{p}}\left(\frac{-i\omega + H_0^\sigma(\mathbf{p})}{Z}\right)\psi_{\sigma,\omega,\mathbf{p}}, \tag{7}$$

$$S_1 = \frac{1}{2}\int \frac{d\omega d^2p}{(2\pi)^3}\Gamma^2 U(\omega,\mathbf{q}) n_{\omega,\mathbf{q}} n_{-\omega,-\mathbf{q}} + S_2. \tag{8}$$

Here the ψ fields are Grassman valued (fermionic) fields with flavour (spin-valley) index σ while ω is a fermionic Matsubara frequency, Γ is a vertex renormalization parameter, Z is the quasiparticle residue, and $n_{\omega,\mathbf{q}}$ is the Fourier transform of the electron density, summed over spins, valleys and sublattices. The effective interaction $U(\omega,\mathbf{q})$ is given by Eq. (4). The term S_2 is included tentatively to represent more complicated interactions that may be generated under RG. In the bare theory, $\Gamma=1$, $Z=1$, and $S_2=0$. The theory is defined with the initial UV cutoff Λ_0. Since the two-band model, Eq. (1), is only justified on energy scales less than the gap $W \approx 0.4$ eV to the higher bands in BLG, we conservatively identify $\Lambda_0 = W$. Our main results will be independent of Λ_0.

As we shall see, the RG flow will inherit the symmetries of the Hamiltonian, Eq. (1), strongly constraining the possible terms S_2. The relevant symmetries are particle-hole symmetry, time reversal symmetry, SU(4) flavour symmetry,[13] and the symmetry of the Hamiltonian under the transformation $e^{i\theta\tau_3}R(\theta/2)$, where $R(\theta)$ generates spatial rotations, $R(\theta)p_\pm = e^{\pm i\theta}p_\pm$.

We will employ an RG scheme which treats frequency ω on the same footing as $p^2/2m$, in order to preserve the form of the free action Eq. (7) under RG. Thus, we integrate out the shell of highest energy fermion modes

$$\Lambda' < \sqrt{\omega^2 + \left(\frac{\mathbf{p}^2}{2m}\right)^2} < \Lambda \tag{9}$$

and subsequently rescale $\omega \to \omega(\Lambda/\Lambda')$, $p \to p(\Lambda/\Lambda')^{1/z}$, where z is the dynamical critical exponent,[9] which takes value $z=2$ at tree level. Because the value $z=2$ is not protected by any symmetry, it may acquire renormalization corrections. However, it will follow from our analysis that the quasiparticle spectrum does not renormalize at leading $\log^2$ order, so that the exponent z does not flow at leading order. We therefore use $z=2$ for the rest of the paper, which corresponds to scaling dimensions $[\omega]=1$ and $[p^2]=1$. Under such an RG transformation, the Lagrangian density in momentum space has scaling dimension $[\mathcal{L}]=2$, and we have tree level scaling dimensions $[\psi]=1/2$ and $[\Gamma]=[Z]=0$, respectively.

Given these tree level scaling dimension values, it can be seen that all potentially relevant terms arising as part of S_2 must involve four fermion fields. Indeed, any term involving more than four ψ fields will be irrelevant at tree level under RG, and may be neglected. The terms with odd numbers of ψ fields are forbidden by charge conservation while the quadratic terms $\Delta_{ij}\psi_i^\dagger\psi_j$ cannot be generated under perturbative RG since they break the symmetries of the Hamiltonian listed above.[17] Thus, the only potentially relevant terms that could arise under perturbative RG take the form of a four-point interaction which may be written as

$$S_2 = \frac{1}{2}\int d^3x d^3x' \Upsilon^{\sigma\sigma'}_{ijkl}\psi^\dagger_{\sigma,i}(x)\psi_{\sigma,j}(x)\psi^\dagger_{\sigma',k}(x')\psi_{\sigma',l}(x'), \tag{10}$$

where $x=(\mathbf{r},t)$, $x'=(\mathbf{r}',t')$. Here Υ is an effective four particle vertex, which is marginal at tree level, the indices σ,σ' refer to the flavour (spin-valley) of the interacting particles, and i,j,k,l are sublattice indices.

The symmetries of the Hamiltonian, Eq. (1), impose strong constraints on the spin-valley-sublattice structure of the four-point vertex Υ. Since the Coulomb interaction does not change fermion flavour (spin or valley), and the electron Green's function is diagonal in flavour space, the vertex Υ cannot change fermion flavour. Moreover, the $SU(4)$ flavour symmetry of the Hamiltonian implies that Υ does not depend on the flavour index of the interacting particles and we may therefore drop the indices σ,σ' in Eq. (10). Finally, the bare Hamiltonian (1) is invariant under combined pseudospin/spatial rotations through $e^{i\theta\tau_3}R(\theta/2)$. This symmetry further restricts the form of four-point vertices in Eq. (10) to have sublattice structure Υ_{iijj} or Υ_{ijji} only.[18] That is, the allowed scattering processes are restricted to $(AA)\to(AA)$, $(AB)\to(AB)$ and $(AB)\to(BA)$. We note that the processes $(AB)\to(AB)$ and $(AB)\to(BA)$ are distinct since the particles have flavour, and the interaction [Eq. (4)] is not short range.

Below we obtain the RG flow for bilayer graphene, working in the manner of Ref. 9. We consider the partition function, Eq. (6), where the interaction is given by Eq. (4). Start-

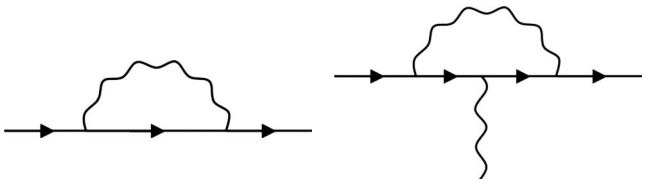

FIG. 1. Diagrammatic representation of (a) self-energy and (b) vertex correction [Eqs. (13) and (27)]. Straight lines with arrows represent fermion propagator, Eq. (12), wavy lines represent dynamically screened long-range interaction, Eq. (4).

ing from this action, supplied with UV cutoff Λ_0, we systematically integrate out the shell of highest energy fermion modes, Eq. (9). We perform the integrals perturbatively in the interaction, Eq. (4). This corresponds to a perturbation theory in small $\Gamma^2 Z^2/N$. We carry out our calculations to one loop order and examine the renormalization, in turn, of the electron Green's function (Sec. IV), the vertex function Γ (Sec. V) and the four-point vertex Y (Sec. VI).

IV. SELF-CONSISTENT RENORMALIZATION OF THE ELECTRON GREEN'S FUNCTION

At first order in the interaction, the fermion Green's function acquires a self-energy Σ, represented diagrammatically (to leading order in the interaction) by Fig. 1(a). A self-consistent expression for the change in the fermion propagator G is

$$\delta G(\omega,\mathbf{q}) = G_0(\omega,\mathbf{q})\Sigma(\omega,\mathbf{q})G_0(\omega,\mathbf{q}), \tag{11}$$

$$G_0(\omega,\mathbf{q}) = \frac{Z_0}{i\omega - H_0(\mathbf{q})}, \tag{12}$$

$$\Sigma(\omega,\mathbf{q}) = -\int \frac{d\varepsilon d^2p}{(2\pi)^3}\Gamma_0^2 U_{\varepsilon,\mathbf{p}} G_0(\varepsilon+\omega,\mathbf{p}+\mathbf{q}), \tag{13}$$

where Σ is a 2×2 matrix in sublattice space.

A number of general properties of the self-energy can be established based on symmetry considerations. It follows from Eq. (13) that $\Sigma(0,0)$ vanishes, since the part of $G(\varepsilon,\mathbf{p})$ which is invariant under rotations of $\mathbf{p}$ is an odd function of frequency ε. Likewise, the expressions for diagonal entries $\Sigma_{AA}(0,\mathbf{q})$ and $\Sigma_{BB}(0,\mathbf{q})$, which involve an integral of an odd function of ε, vanish on integration over ε. For the same reason, the expressions for off-diagonal entries $\Sigma_{AB}(\omega,0)$ and $\Sigma_{BA}(\omega,0)$ vanish upon integrating the momentum $\mathbf{p}$ over angles. Hence, nonvanishing contributions arise at lowest order when the right hand side of Eq. (13) is expanded to leading order in small ω and $\mathbf{q}$. We obtain

$$\Sigma_{AA}(\omega,\mathbf{q}) = -i\omega\frac{i\,\partial\Sigma_{AA}(0,0)}{\partial\omega} + O(\omega^2,\omega q^2,q^4), \tag{14}$$

$$\Sigma_{AB}(\omega,\mathbf{q}) = \frac{\mathbf{q}_+^2}{2m}\frac{\partial\Sigma_{AB}(0,0)}{\partial(q_+^2/2m)} + O(\omega^2,\omega q^2,q^4), \tag{15}$$

where $\Sigma_{AA}=\Sigma_{BB}$ and $\Sigma_{AB}=\Sigma_{BA}^*$ by symmetry.

It was shown in Ref. 7 that $i\partial\Sigma_{AA}/\partial\omega$ and $\partial\Sigma_{AB}/\partial(q_+^2/2m)$ are both $\log^2$ divergent, and are equal to leading order (see below and Sec. VIII for alternative derivation). Thus the self-energy can be written, with logarithmic accuracy, as

$$\Sigma(\omega,\mathbf{q}) = -iZ_0\frac{\partial\Sigma}{\partial\omega}G_0^{-1}(\omega,\mathbf{q}) + O\left(\ln\frac{\Lambda}{\Lambda'}\right). \tag{16}$$

Here, it is understood that nonvanishing $\partial\Sigma/\partial\omega$ is due to the modes that have been integrated out, Eq. (9). Within the leading log approximation, the electron Green's function, Eq. (12), retains its noninteracting form, whereby the self-energy, upon substitution into Eq. (11), can be absorbed entirely into a redefinition of the quasiparticle residue, as

$$\delta G(\omega,\mathbf{q}) = \frac{1}{i\omega - H_0(\mathbf{q})}\delta Z, \quad \delta Z = -i\frac{\partial\Sigma_{AA}}{\partial\omega}Z_0^2. \tag{17}$$

We emphasize that the lack of renormalization of the mass only holds at $\log^2$ order. The subleading single log renormalization of the mass will be analyzed in Sec. VIII.

The renormalization of the quasiparticle residue, Eq. (17), can be evaluated explicitly by calculating $i\partial\Sigma/\partial\omega$. Taking Σ from Eq. (13), we write

$$i\frac{\partial\Sigma}{\partial\omega}\bigg|_{\omega=0} = -\int \frac{d\varepsilon d^2p}{(2\pi)^3}\frac{\left(\frac{p^2}{2m}\right)^2-\varepsilon^2}{\left[\left(\frac{p^2}{2m}\right)^2+\varepsilon^2\right]^2}\frac{2\pi\Gamma_0^2 Z_0 e^2}{\kappa p - 2\pi e^2\Pi\left(\frac{2m\varepsilon}{p^2}\right)}. \tag{18}$$

We express the momenta in polar coordinates $p_x=p\cos\alpha$, $p_y=p\sin\alpha$, and straightaway integrate over $-\pi<\alpha<\pi$. We further change to pseudopolar coordinates in the frequency-momentum space, $\varepsilon=r\cos\theta$, $p^2/2m=r\sin\theta$, with the "polar angle" $0<\theta<\pi$. Using the Rydberg energy E_0, Eq. (3), as units for r, we have

$$i\frac{\partial\Sigma}{\partial\omega} = -\int_{\Lambda'}^{\Lambda}\frac{dr}{r}\int_0^{\pi}\frac{d\theta}{2\pi}\frac{(\sin^2\theta-\cos^2\theta)\Gamma_0^2 Z_0}{\sqrt{2r\sin\theta}-\frac{2\pi}{m}\Pi(\theta)}, \tag{19}$$

where $\Pi(\theta)$ is the dimensionless polarization function, given by Eq. (5) with quasiparticle mass m suppressed and $2m\varepsilon/p^2=\cot\theta$. We note that $\Pi(\theta)$ goes to zero when $\theta\to 0,\pi$, and these zeros of the polarization function dominate the integral and lead to the $\log^2$ divergence. Since $\Pi(\theta)$ is even about $\theta=\pi/2$, the $\log^2$ contribution can be evaluated by replacing $\Pi(\theta)$ in Eq. (19) by its asymptotic $\theta\ll\pi$ form,

$$\Pi(\theta) \approx \frac{Nm}{4}\tan\theta. \tag{20}$$

In the region $\theta\ll\pi$, we may approximate $\sin\theta\approx\theta$, $\tan\theta\approx\theta$, and $\cos\theta\approx 1$. Including a factor of 2 for the region $\theta\approx\pi$, which gives a contribution identical to that of the region $\theta\approx 0$, we can express the integral Eq. (19) with logarithmic accuracy as

$$i\frac{\partial\Sigma}{\partial\omega}=2\int_{\Lambda'}^{\Lambda}\frac{dr}{r}\int_{0}^{\pi/2}\frac{d\theta}{2\pi}\frac{\Gamma_0^2Z_0}{\sqrt{2r\theta}+\frac{N\pi}{2}\theta}. \tag{21}$$

Performing the integral over θ and assuming $r \ll N^2$, yields

$$i\frac{\partial\Sigma}{\partial\omega}=\frac{2\Gamma_0^2Z_0}{N\pi^2}\int_{\Lambda'}^{\Lambda}\frac{dr}{r}\ln\frac{N^2\pi^2}{8r}. \tag{22}$$

Integrating over $\Lambda' < r < \Lambda$ [see Eq. (9)], we obtain

$$i\frac{\partial\Sigma}{\partial\omega}=\frac{2\Gamma_0^2Z_0}{N\pi^2}\left(\ln\frac{N^2\pi^2E_0}{8\Lambda'}\ln\frac{\Lambda}{\Lambda'}-\frac{1}{2}\ln^2\frac{\Lambda}{\Lambda'}\right). \tag{23}$$

We now consider an infinitesimal RG transformation. Defining an RG time

$$\xi=\ln\frac{\Lambda_0}{\Lambda},\quad \delta\xi=\ln\frac{\Lambda}{\Lambda'}, \tag{24}$$

we rewrite the recursion relation, Eq. (23), as

$$i\frac{\partial\Sigma}{\partial\omega}=\frac{2\Gamma_0^2Z_0}{N\pi^2}(\xi+c)d\xi,\quad c=\ln\frac{N^2\pi^2E_0}{8\Lambda_0}. \tag{25}$$

The constant term c describes corrections subleading in $\log^2$, and thus may seem to be irrelevant. However, we shall retain it in the RG equation since it will determine the form of renormalization near the UV cutoff (see discussion of TDOS in Sec. VII).

In our derivation of Eq. (22) it was assumed that our initial UV cutoff $\Lambda_0 < N^2\pi^2E_0/8$. Such choice of Λ_0 is certainly justified when N is large, which is the limit we worked on thus far. Better still, this condition remains entirely reasonable for the physical value $N=4$, leading to $N^2\pi^2E_0/8=24\ eV\kappa^{-2}$, which is much bigger than the bandwidth for BLG.

Substituting Eq. (25) into Eq. (17), we obtain a differential equation for the flow of the quasiparticle residue,

$$\frac{\partial Z}{\partial\xi}=-\frac{2\Gamma^2(\xi)Z^3(\xi)}{N\pi^2}(\xi+c). \tag{26}$$

This equation encapsulates a one loop RG flow for the residue Z, describing its renormalization within a $\log^2$ accuracy.

V. SELF-CONSISTENT RENORMALIZATION OF THE VERTEX FUNCTION Γ

The screened Coulomb interaction renormalizes through the vertex correction, pictured in Fig. 1(b). The RPA bubble diagrams, which have already been taken into account in moving from an unscreened to a screened interaction, Eq. (4), do not contribute to renormalization. It may be verified by an explicit calculation that the vertex correction in Fig. 1(b) is given by

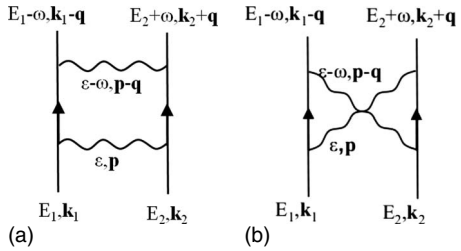

FIG. 2. The renormalization of the four-point vertex Υ proceeds through repeated scattering in (a) the particle-particle channel and in (b) the particle-hole channel, known as the BCS loop and the ZS′ loop in the Luttinger liquid literature (Ref. 9). The RPA bubble diagrams (ZS loop in the language of Ref. 9), which arise in the same order of perturbation theory, have already been taken into account in the screened interaction, Eq. (4).

$$\delta\Gamma=-\int\frac{d\varepsilon d^2p}{(2\pi)^3}\frac{\left(\frac{p^2}{2m}\right)^2-\varepsilon^2}{\left[\left(\frac{p^2}{2m}\right)^2+\varepsilon^2\right]^2}\frac{2\pi\Gamma_0^3Z_0^2e^2}{\kappa p-2\pi e^2\Pi\left(\frac{2m\varepsilon}{p^2}\right)}. \tag{27}$$

This is the same expression as for the residue renormalization [Eqs. (17) and (18)], with Γ replacing Z, and a sign change. Hence, we obtain

$$\frac{\partial\Gamma}{\partial\xi}=\frac{2\Gamma^3(\xi)Z^2(\xi)}{N\pi^2}(\xi+c) \tag{28}$$

which is identical to the flow equation for Z, albeit with a reversed sign. Therefore, the product ΓZ does not renormalize at log square order, and we can write

$$\Gamma(\xi)Z(\xi)=1. \tag{29}$$

This result is not a coincidence since the residue Z and the vertex function Γ are not independent quantities. The Hamiltonian, Eq. (1), is invariant under a gauge transformation of electron wave function $\psi'=\psi e^{i\chi}$, accompanied by energy and momentum shifts $\varepsilon'=\varepsilon-\partial_t\chi$, $\mathbf{p}'=\mathbf{p}+\nabla\chi$. This gauge invariance symmetry can be shown to lead to Eq. (29) through a Ward identity that relates the self-energy to the vertex function.[19,20]

VI. RENORMALIZATION OF THE FOUR-POINT VERTEX Υ

The four-point vertex Υ, introduced in Eq. (10), renormalizes through the diagrams presented in Figs. 2(a) and 2(b), which represent the repeated scattering of two particles in the electron-electron and electron-hole channels, respectively. We follow the naming conventions used in Ref. 9 in the context of the Luttinger liquid, and name these two diagrams, the BCS loop and the ZS' loop, pictured in Figs. 2(a) and 2(b), respectively. In the one dimensional Luttinger liquids, the two processes famously cancel,[8] so that the four-point vertex does not renormalize. In higher dimensions, such a cancellation is rare. However, the discrete nature of the Fermi surface in BLG results in a Luttinger liquid-

like cancellation of the processes Figs. 2(a) and 2(b), as will be discussed below.

We argued in Sec. III that the RG-relevant scattering processes allowed by symmetry must have sublattice structure $(A,A)\to(A,A)$, $(A,B)\to(A,B)$, or $(A,B)\to(B,A)$. To see the mathematical origin of such selection, it is instructive to explicitly write out the form of the electron Green's function. We have

$$G_{AA}(\varepsilon,\mathbf{p}) = \frac{-Zi\varepsilon}{\varepsilon^2 + (p^2/2m)^2} = G_{BB}(\varepsilon,\mathbf{p}), \tag{30}$$

$$G_{AB}(\varepsilon,\mathbf{p}) = \frac{-Zp_+^2/2m}{\varepsilon^2 + (p^2/2m)^2} = G^*_{BA}(\varepsilon,\mathbf{p}). \tag{31}$$

When the diagrams Figs. 2(a) and 2(b) are evaluated in any channel other than these three channels, they vanish upon integration over inner momentum variables, due to the chiral structure of the sublattice changing Green's functions, Eq. (31).

Similar reasoning leads to a conclusion that the $(A,B)\to(B,A)$ vertex cannot exhibit a $\log^2$ divergence. As we saw above, the $\log^2$ divergences arise because the effective interaction $U_{\varepsilon,\mathbf{p}}$ has a pole at $\mathbf{p}=0$ and finite ε. However, the sublattice changing Green's functions, Eq. (31), have zeros at small $\mathbf{p}$, which cancel the contribution of the pole in the interaction. Thus, the diagrams in Fig. 2 can only be $\log^2$ divergent if all internal Green's functions are sublattice preserving, given by Eq. (30). Since the process $(AB)\to(BA)$ involves two sublattice changing Green's functions, it follows that the integrals associated with this processes cannot be $\log^2$ divergent, and hence this process does not contribute at leading $\log^2$ order.

Thus, at leading order, we need to consider only the processes $(AA)\to(AA)$ and $(AB)\to(AB)$. Moreover since the interaction [Eq. (4)] does not distinguish between sublattices, the ZS′ and BCS contributions from Figs. 2(a) and 2(b) in these channels are the same. Therefore, to demonstrate that Υ does not renormalize at leading order, it is sufficient to demonstrate that there are no $\log^2$ divergences in the $(AA)\to(AA)$ channel.

In evaluating the ZS′ and BCS diagrams (Fig. 2), it will prove important to keep track of external momenta. The vertex $\Upsilon(E_1,E_2,\omega,\mathbf{k}_1,\mathbf{k}_2,\mathbf{q})$ then represents the amplitude for the scattering process

$$\psi_{\sigma,A,E_1,\mathbf{k}_1}\psi_{\sigma',A,E_2,\mathbf{k}_2} \to \psi_{\sigma,A,E_1+\omega,\mathbf{k}_1+\mathbf{q}}\psi_{\sigma',A,E_2-\omega,\mathbf{k}_2-\mathbf{q}}.$$

Translating the ZS′ and BCS diagrams in Fig. 2 into integrals, we find the contributions

$$\Upsilon^{ZS'}_{AAAA} = \Gamma^4 \int \frac{d\varepsilon d^2p}{(2\pi)^3} U_{\varepsilon,\mathbf{p}} U_{\varepsilon-\omega,\mathbf{p}-\mathbf{q}} G_{AA}(E_1+\varepsilon,\mathbf{k}_1+\mathbf{p}) \times G_{AA}(E_2+\varepsilon-\omega,\mathbf{k}_2+\mathbf{p}-\mathbf{q}), \tag{32}$$

$$\Upsilon^{BCS}_{AAAA} = \Gamma^4 \int \frac{d\varepsilon d^2p}{(2\pi)^3} U_{\varepsilon,\mathbf{p}} U_{\varepsilon-\omega,\mathbf{p}-\mathbf{q}} G_{AA}(E_1+\varepsilon,\mathbf{k}_1+\mathbf{p}) \times G_{AA}(E_2-\varepsilon,\mathbf{k}_2-\mathbf{p}). \tag{33}$$

Here, the interaction $U(\varepsilon,p)$ is defined by Eq. (4), the Green's functions are defined by Eq. (30), and the integral goes over the shell defined by Eq. (9).

As always in a RG analysis, we assume that the external frequencies and momenta are small compared to the internal frequencies and momenta

$$\max\left(\omega,\omega',\frac{\mathbf{q}^2}{2m},\frac{\mathbf{q}'^2}{2m}\right) \ll \Lambda' < \sqrt{\varepsilon^2 + \left(\frac{\mathbf{p}^2}{2m}\right)^2} < \Lambda. \tag{34}$$

In such a case, the standard approach to handling the integrals over ε and $\mathbf{p}$ involves setting the external frequency and momenta to zero at first, and restoring their finite values later to regulate the infrared (IR) divergences. However, a straightforward application of this recipe to the integrals in Eqs. (32) and (33) proves impossible, because these integrals are power law divergent when all external momenta are set to zero. The divergence arises from the region near $\mathbf{p}\approx 0$ [which lies within the shell defined by Eq. (9)], where the interaction is nearly unscreened. In this region, we have

$$U_{\varepsilon,\mathbf{p}} U_{\varepsilon-\omega,\mathbf{p}-\mathbf{q}} \sim \frac{1}{(|\mathbf{p}| + \alpha|\mathbf{p}|^2)(|\mathbf{p}-\mathbf{q}| + \alpha|\mathbf{p}-\mathbf{q}|^2)} \tag{35}$$

with $\alpha = Ne^2/2\kappa\varepsilon$. At finite $\mathbf{q}$, the poles in this expression are split apart, and thus the singular contribution of each pole, $\mathbf{p}=0$ and $\mathbf{p}=\mathbf{q}$, is regularized by the integration measure d^2p so that the integrals in Eqs. (32) and (33) remain well defined. However, when all external momenta are zero, the poles from the two interaction lines coincide, and the expressions (32) and (33) acquire a second-order pole at $\mathbf{p}=0$. When we integrate over this second-order pole, we pick up a power law divergence.

Hence, if either of the ZS′ or BCS diagrams existed in isolation, this power law divergence would indicate a strong (power law) instability, which would drive Υ into the strong coupling regime, where our $\log^2$ RG would cease to apply. However, as we will now show, the divergences in the contributions to Υ from the expressions (32) and (33) in fact cancel out, so that Υ does not flow to $\log^2$ order. To analyze the cancellation between the ZS′ and BCS diagrams, it is convenient to add the integrands of Eqs. (32) and (33) together before doing the integral while keeping external momenta finite. Preserving finite external momenta ensures that the integrals Eqs. (32) and (33) are well defined. After combining the integrands and denoting $\Upsilon^{ZS'}_{AAAA} + \Upsilon^{BCS}_{AAAA} = \tilde{\Upsilon}$, we obtain

$$\tilde{\Upsilon} = \Gamma^4 \int \frac{d\varepsilon d^2p}{(2\pi)^3} U_{\varepsilon,\mathbf{p}} U_{\varepsilon-\omega,\mathbf{p}-\mathbf{q}} G_{AA}(E_1+\varepsilon,\mathbf{k}_1+\mathbf{p}) \times [G_{AA}(E_2+\varepsilon-\omega,\mathbf{k}_2+\mathbf{p}-\mathbf{q}) + G_{AA}(E_2-\varepsilon,\mathbf{k}_2-\mathbf{p})]. \tag{36}$$

To simplify this expression we note that momentum $\mathbf{q}$ enters very differently in Eq. (36) as compared to other external frequencies and momenta E_1, E_2, ω, $\mathbf{k}_1$, and $\mathbf{k}_2$. The momentum $\mathbf{q}$ is needed to split the poles coming from the two interaction terms—if we take $\mathbf{q}$ to zero, the integral will acquire a second-order pole at $\mathbf{p}=0$, leading to a divergence. This divergence arises from within the shell that we are integrating out [Eq. (9)], and thus the RG will be ill defined. In contrast, sending the frequencies and momenta E_1, E_2, ω, $\mathbf{k}_1$, and $\mathbf{k}_2$ to zero by applying Eq. (34) does not cause any concern. We thus have

$$\tilde{\Upsilon} = \Gamma^4 \int \frac{d\varepsilon d^2p}{(2\pi)^3} U_{\varepsilon,\mathbf{p}} U_{\varepsilon,\mathbf{p}-\mathbf{q}} G_{AA}(\varepsilon,\mathbf{p}) \times [G_{AA}(\varepsilon,\mathbf{p}-\mathbf{q}) + G_{AA}(-\varepsilon,-\mathbf{p})]. \quad (37)$$

Interestingly, the expression in square brackets vanishes identically when $\mathbf{q}=0$ since $G_{AA}(\varepsilon,\mathbf{p})=-G_{AA}(-\varepsilon,-\mathbf{p})$. However, taking the limit $\mathbf{q}\to 0$ is potentially problematic because of the pole structure of $U_{\varepsilon,\mathbf{p}}U_{\varepsilon-\omega,\mathbf{p}-\mathbf{q}}$ discussed above. Instead, we proceed with caution and evaluate Eq. (37) at finite $\mathbf{q}$, using the conditions [Eq. (34)] to simplify the analysis.

Given what we just said, it is now easy to see why there is no $\log^2$ divergence in $\tilde{\Upsilon}$. First, we note that the interaction Eq. (4) carries a soft UV cutoff, so the integral in Eq. (37) is UV convergent (this property of dynamically screened interaction in BLG is discussed, e.g., in Ref. 3). Hence, we can shift variables to $\mathbf{p}_\pm=\mathbf{p}\pm\mathbf{q}/2$ and rewrite the expression (37) as

$$\begin{aligned}\tilde{\Upsilon} &= -\Gamma^4 Z^2 \int \frac{d\varepsilon d^2p}{(2\pi)^3} U_{\varepsilon,\mathbf{p}_+} U_{\varepsilon,\mathbf{p}_-} \varepsilon^2 D(\varepsilon,\mathbf{p}_+)[D(\varepsilon,\mathbf{p}_-) - D(\varepsilon,\mathbf{p}_+)] \\ &= -\Gamma^4 Z^2 \int \frac{d\varepsilon d^2p}{(2\pi)^3} U_{\varepsilon,\mathbf{p}_+} U_{\varepsilon,\mathbf{p}_-} \varepsilon^2 \left[\frac{D(\varepsilon,\mathbf{p}_+)+D(\varepsilon,\mathbf{p}_-)}{2} + \frac{D(\varepsilon,\mathbf{p}_+)-D(\varepsilon,\mathbf{p}_-)}{2} \right] [D(\varepsilon,\mathbf{p}_-) - D(\varepsilon,\mathbf{p}_+)], \end{aligned} \quad (38)$$

where we factored the Green's functions as

$$G_{AA}(\varepsilon,p) = iZ\varepsilon D(\varepsilon,\mathbf{p}), \quad D(\varepsilon,\mathbf{p}) = \frac{1}{\varepsilon^2 + (\mathbf{p}^2/2m)^2}. \quad (39)$$

We note that because Υ should be even under $\mathbf{q}\to-\mathbf{q}$ the first term in the brackets gives zero upon integration over $\mathbf{p}$. Hence, we can rewrite the result for $\tilde{\Upsilon}$, Eq. (38), as

$$\begin{aligned}\tilde{\Upsilon} &= \frac{\Gamma^4 Z^2}{2} \int \frac{d\varepsilon d^2p}{(2\pi)^3} U_{\varepsilon,\mathbf{p}_+} U_{\varepsilon,\mathbf{p}_-} \varepsilon^2 [D(\varepsilon,\mathbf{p}_-) - D(\varepsilon,\mathbf{p}_+)]^2 \\ &= \frac{\Gamma^4 Z^2}{2} \int \frac{d\varepsilon d^2p}{(2\pi)^3} U_{\varepsilon,\mathbf{p}_+} U_{\varepsilon,\mathbf{p}_-} \varepsilon^2 \left[\frac{z_+^2 - z_-^2}{(\varepsilon^2+z_+^2)(\varepsilon^2+z_-^2)} \right]^2, \end{aligned} \quad (40)$$

where $z_\pm=|\mathbf{p}_\pm|^2/2m$.

To extract the leading contribution at small $\mathbf{q}$, we approximate the effective interaction as

$$U(\varepsilon,\mathbf{p}) = -\frac{\Pi^{-1}(\varepsilon,\mathbf{p})}{1-\frac{\kappa|\mathbf{p}|}{2\pi e^2\Pi(\varepsilon,\mathbf{p})}} \approx -\frac{1}{\Pi(\varepsilon,\mathbf{p})}. \quad (41)$$

From the definition of the polarization function, Eq. (5), we see that the approximation $U\approx -1/\Pi$ holds everywhere in the shell Eq. (9) except at $\mathbf{p}\approx 0$ since $\Pi(\mathbf{p}=0)=0$. However, in the limit $\mathbf{p}\to 0$, the expression in brackets in Eq. (40) tends to zero because of the expansion $z_+^2-z_-^2=(\mathbf{p}^2/m)(\mathbf{p}\cdot\mathbf{q}/2m)+O(\mathbf{p}^4)$, which ensures validity of the approximation [Eq. (41)].

Hence, using Eq. (5), we obtain

$$\tilde{\Upsilon} = \Gamma^4 Z^2 \int d\varepsilon d^2p \frac{\sqrt{(z_+^2+u\varepsilon^2)(z_-^2+u\varepsilon^2)}}{4\pi(Nm\ln 4)^2} \times \frac{\varepsilon^2}{z_+z_-}\left[\frac{z_+^2-z_-^2}{(\varepsilon^2+z_+^2)(\varepsilon^2+z_-^2)}\right]^2. \quad (42)$$

Simple power counting shows that this integral is UV convergent, IR convergent, and is completely independent of q, which can be scaled out by defining new variables $p'=p/q$ and $\varepsilon'=2m\varepsilon/q^2$. It follows that the diagrams representing repeated scattering in the particle-particle and particle-hole channels do indeed cancel, so that $\Upsilon_{AAAA}Z^2$ does not renormalize.

Combining this with our argument demonstrating that $\Upsilon_{ABBA}Z^2$ does not renormalize at $\log^2$ order [see discussion below Eq. (31)], and recalling that $\Upsilon_{AAAA}=\Upsilon_{AABB}$, we conclude that we can set $\Upsilon=0$ with $\log^2$ accuracy.

VII. SOLUTION OF RG FLOW EQUATIONS. ZERO BIAS ANOMALY IN BILAYER GRAPHENE

Since the only quantities which renormalize at $\log^2$ order in a one loop RG are the quasiparticle residue Z and the interaction vertex function Γ, the problem of finding the RG flow of these quantities reduces to solving Eqs. (26) and (28). All other quantities do not renormalize at log square order, and may thus be treated as constants with logarithmic accuracy.

Additional simplification arises due to the Ward identity $\Gamma Z=1$, Eq. (29). Using it to decouple the RG equations for Z and Γ, we write the equation for Z as

$$\frac{\partial Z}{\partial \xi} = -\frac{2}{\pi^2 N}(\xi + c)Z, \quad (43)$$

where we retained a constant $c=\ln\frac{N^2\pi^2E_0}{8\Lambda_0}$ corresponding to the first term in the self-energy renormalization, Eq. (23).

Integrating the RG equation, and taking into account the boundary conditions $Z(0)=\Gamma(0)=1$, we obtain

$$Z(\xi) = \exp\left(-\frac{2c\xi+\xi^2}{N\pi^2}\right) = \Gamma^{-1}(\xi), \quad \xi = \ln\frac{\Lambda_0}{\Lambda}. \quad (44)$$

We note that in the limit of small ξ^2/N, we reproduce the perturbative result[7] for the residue, Eq. (23). However, our

result [Eq. (44)] applies for all ξ, both small and large. The fermion propagator at arbitrary energies and momenta is then given by

$$G(\omega,\mathbf{k}) = -Z(\xi)\frac{i\omega + H_0(\mathbf{k})}{\omega^2 + \left(\frac{\mathbf{k}^2}{2m}\right)^2}. \tag{45}$$

At zero temperature, the infrared cutoff is supplied by the external frequency and momentum, such that $\xi = \ln\frac{\Lambda_0}{\Lambda}$ and $\Lambda = \sqrt{\omega^2 + (k^2/2m)^2}$

Thus, the quasiparticle residue in undoped BLG is suppressed to zero by electron-electron interactions, Eq. (45). This is reminiscent of the situation in disordered metals, where enhancement of interactions by disorder produces a renormalization of electron self-energy of a $\log^2$ form,[11] and analysis of an RG flow[12] yields a suppression of the quasiparticle residue similar in form to our Eq. (45). The suppression of the quasiparticle spectral weight at low energies, governed by the $Z(\xi)$ dependence, will manifest itself directly in the behavior of the tunneling density of states of BLG, similar to disordered metals.

We note parenthetically that while keeping the constant term c in the RG Eq. (43) is formally beyond the $\log^2$ accuracy generally adopted in our analysis, it can be justified on the same grounds as in the discussion of the zero bias anomaly in disordered metals.[21,22] Because of its fairly large value for $N=4$, given by $c = \ln 2\pi^2 \approx 2.98$, this term may significantly alter predictions for the behavior of Z at intermediate energies $\varepsilon \lesssim \Lambda_0$.

To analyze the suppression of TDOS, we use its relation to the retarded Green's function,[11]

$$\rho(\omega) = -\frac{1}{\pi}\mathrm{Im}[\mathrm{Tr}\, G_R(\omega,\mathbf{k})], \tag{46}$$

where $G_R(\omega,\mathbf{k})$ is obtained from the Matsubara Green's function analyzed above, Eq. (45), by the analytic continuation of frequency from imaginary to real values, $i\omega \to \omega + i\eta$.

It is convenient to take the trace before performing the analytic continuation. The trace may be most easily taken in a basis of free particle eigenstates (plane waves with appropriate spinor structure), which amounts to integrating Eq. (45) over all $\mathbf{k}$ values, $\mathrm{Tr}\, G = \int G(\omega,\mathbf{k}) d^2k$. Noting that the term containing $H_0(\mathbf{k})$ vanishes upon integration due to the angular dependence, we write

$$\mathrm{Tr}\, G = 2\frac{N_0}{\pi}\int_0^\infty Z(\xi)\frac{i\omega}{\omega^2 + z^2}dz, \tag{47}$$

where $z = \mathbf{k}^2/2m$ and N_0 is the density of electronic states in BLG in the absence of interactions.

It can be seen that the integral over z is determined by $z \sim \omega$. It is therefore convenient to introduce a variable $\varphi = \sinh^{-1}(z/\omega)$ and write

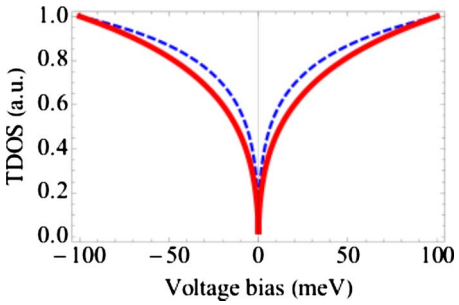

FIG. 3. (Color online) TDOS of BLG at charge neutrality, Eq. (51), is shown as a function of external bias $\omega = eV$. Predicted TDOS is shown for two different values of the dielectric constant in E_0, Eq. (3): $\kappa = 1$ (solid curve) and $\kappa = 2.5$ (dashed curve), describing free-standing BLG and BLG on SiO substrate, respectively. Plot is normalized so that $\rho = 1$ at an external bias of 100 meV.

$$\mathrm{Tr}\, G = i\frac{N_0}{\pi}\int_0^\infty Z(\xi_\omega - \ln\cosh\varphi)\frac{d\varphi}{\cosh\varphi}, \tag{48}$$

where $\xi_\omega = \ln(\Lambda_0/\omega)$. Noting that this integral is dominated by $\varphi \sim 1$, we obtain an estimate of the spectral weight

$$\rho(\omega) \approx N_0 Z(\xi_\omega) = N_0 \exp\left(-\frac{\xi_\omega^2 + 2c\xi_\omega}{N\pi^2}\right). \tag{49}$$

The form of this expression remains unchanged, to leading $\log^2$ order, upon analytic continuation to real frequencies.

The expression in Eq. (49) can be rearranged by using Eq. (25) as

$$\rho(\omega) = N_0 \exp\left(-\frac{\ln^2\frac{N^2\pi^2 E_0}{8\omega} - \ln^2\frac{N^2\pi^2 E_0}{8\Lambda_0}}{N\pi^2}\right). \tag{50}$$

Thus, we see that the only effect of the UV cutoff Λ_0 is to rescale the prefactor for the TDOS without affecting the frequency dependence. Absorbing the dependence on Λ_0 in the prefactor,

$$\rho(\omega) = \tilde{N}_0 \exp\left(-\frac{1}{N\pi^2}\ln^2\frac{N^2\pi^2 E_0}{8\omega}\right). \tag{51}$$

Tunneling measurements yield $\rho(\omega = eV)$, where V is the bias voltage. The interaction suppression of the density of states, Eq. (49), will therefore manifest itself as a zero bias anomaly in tunneling experiments. The predicted behavior of the TDOS is shown in Fig. 3. Because of the exponential dependence in Eq. (51), the suppression rapidly becomes more pronounced at lower energies.

Closing our discussion of the zero bias anomaly in BLG, we note that the results described above apply only to the system at charge neutrality. Away from neutrality, with the Fermi surface size becoming finite, the effects of screening will grow stronger, resulting in a weaker effective interaction. Yet, even in this case, the tunneling density of states will be described by the suppression factor $\rho(\omega = eV)/N_0$ given by Eq. (49), provided that the bias voltage eV exceeds the Fermi energy measured from the neutrality point.

VIII. SINGLE LOG RENORMALIZATION OF ELECTRON MASS

Thus far we have concentrated on $\log^2$ flows. However, the analysis may be extended to obtain the subleading single log flows of the action. We illustrate this procedure by calculating the renormalization of the mass (which did not renormalize at $\log^2$ order in the RG). This calculation is interesting because it allows us to investigate the interaction renormalization of the compressibility—a directly measurable quantity and also because it allows us to illustrate how much slower the single log flows are than the $\log^2$ flows.

In this section, we first analyze mass renormalization by extracting it directly from the self-energy. After that, in Sec. IX we consider electron compressibility of BLG and show that the log divergent correction to the compressibility matches exactly our prediction for mass renormalization obtained from the self-energy.

In BLG, the self-energy is a 2×2 matrix, given by Eq. (13), which is related to the renormalized Green's function by the Dyson equation,

$$G^{-1}(\omega,\mathbf{q}) = G_0^{-1}(\omega,\mathbf{q}) - \begin{bmatrix} \Sigma_{AA}(\omega,\mathbf{q}) & \Sigma_{AB}(\omega,\mathbf{q}) \\ \Sigma_{BA}(\omega,\mathbf{q}) & \Sigma_{BB}(\omega,\mathbf{q}) \end{bmatrix}. \quad (52)$$

As discussed in Sec. IV, the leading $\log^2$ contribution to the self-energy is proportional to G_0^{-1} since $\partial\Sigma_{AB}/\partial(q_+^2/2m) = i\partial\Sigma_{AA}/\partial\omega$. This means that all renormalization can be attributed to the residue Z with mass remaining unchanged. However, as we now show, this equality is only true to leading logarithmic order.

Comparison of Eq. (52) with Eqs. (14) and (15) indicates that the mass renormalization is given by

$$\frac{\delta m}{m} = Z_0\left[i\frac{\partial\Sigma_{AA}}{\partial\omega} - \frac{\partial\Sigma_{AB}}{\partial(q_+^2/2m)}\right]. \quad (53)$$

Here, $i\partial\Sigma_{AA}/\partial\omega$ is defined by Eq. (18). For the second term, we obtain the expression

$$\frac{\partial\Sigma_{AB}}{\partial(q_+^2/2m)} = \int \frac{d\varepsilon d^2p}{(2\pi)^3}\left\{ \frac{1}{\varepsilon^2+\left(\frac{p^2}{2m}\right)^2} - \frac{5\left(\frac{p^2}{2m}\right)^2}{\left[\varepsilon^2+\left(\frac{p^2}{2m}\right)^2\right]^2} + \frac{4\left(\frac{p^2}{2m}\right)^4}{\left[\varepsilon^2+\left(\frac{p^2}{2m}\right)^2\right]^3}\right\}\Gamma^2 Z U(\varepsilon,\mathbf{p}), \quad (54)$$

where $U(\varepsilon,\mathbf{p})$ is given by Eq. (4). To evaluate the difference in Eq. (53), it is convenient to subtract the integrands of Eqs. (18) and (54) before doing the integrals. Once again, we use the "polar" representation of the frequency and momentum variables, $\omega = r\cos\theta$, $p^2/2m = r\sin\theta$, and obtain

$$\frac{\delta m}{m} = \int_{\Lambda'}^{\Lambda}\frac{dr}{r}\int_0^{\pi}\frac{d\theta}{2\pi}\frac{\Gamma_0^2 Z_0^2(3\sin^2\theta - 4\sin^4\theta)}{\sqrt{2r\sin\theta} - 2\pi\Pi(\theta)},$$

where $\Pi(\theta)$ is the dimensionless polarization function introduced in Eq. (19) and r is measured in units of E_0 as before. The integral over θ is now fully convergent and the resulting expression is only single log divergent. Integrating analytically over r and then integrating numerically over θ, we find

$$\frac{\delta m}{m} = \frac{0.56}{2N\pi\ln 4}\Gamma_0^2 Z_0^2 \ln\frac{\Lambda}{\Lambda'}. \quad (55)$$

Converting this recursion relation into a differential equation, we obtain

$$\frac{d\ln m}{d\xi} = \frac{0.56}{2N\pi\ln 4}\Gamma^2 Z^2. \quad (56)$$

This equation cannot be solved for general ξ by applying the Ward identity Eq. (29) since the Ward identity only holds at leading $\log^2$ order while the mass flows at subleading (single log) order in Eq. (56). In the perturbative limit $\frac{1}{N}\xi \ll 1$, when $Z\approx 1$ and $\Gamma\approx 1$, from Eq. (56) we obtain a logarithmic correction to the mass

$$m(\xi) = m(0)\left(1 + \frac{0.56}{2N\pi\ln 4}\xi\right). \quad (57)$$

We may relate this mass renormalization to a measurable quantity, by noting that the electronic compressibility K is proportional to the density of states which is proportional to the mass. Thus, the logarithmic renormalization of the mass in Eq. (57) should manifest itself in a logarithmic enhancement of the electronic compressibility. The relation between mass renormalization and compressibility will be further discussed in Sec. IX.

IX. INTERACTION CORRECTION TO COMPRESSIBILITY

Here we explicitly calculate the renormalization of the compressibility. By doing this we shall confirm that the compressibility does not renormalize at leading (log square) order and also extract the single log renormalization of the compressibility. The interaction correction to the compressibility K is given by

$$\delta K = -\frac{\partial^2 F}{\partial\mu^2}, \quad (58)$$

where μ is the chemical potential, and F is the interaction energy. Within the RPA framework, the interaction energy is expressed as

$$F(\mu) = \int\frac{d\omega d^2p}{(2\pi)^3}\ln[1 - V(\mathbf{q})\Pi(\mu,\omega,\mathbf{q})]. \quad (59)$$

Here, $\Pi(\mu,\omega,\mathbf{q})$ is the noninteracting polarization function evaluated at a chemical potential μ and $V(q)$ is the unscreened Coulomb interaction $V(q) = 2\pi e^2/\kappa q$.

To evaluate the second derivative in [Eq. (58)], we consider the difference $\Delta F = F(\mu) - F(0)$. After rearranging logs under the integral, we rewrite this expression as

$$\Delta F = -\int \frac{d\omega d^2q}{(2\pi)^3} \ln[1 - U_{\omega,q}(\Pi(\mu,\omega,q) - \Pi(0,\omega,q))], \tag{60}$$

where now $U_{\omega,q}$ is the dynamically screened Coulomb interaction, Eq. (4). Since the compressibility is obtained from the free energy through $K=-\partial^2 F/\partial\mu^2$, the problem of calculating the interaction renormalization of the compressibility is reduced to that of calculating the polarization function at finite μ. This may be calculated through methods similar to those developed in Ref. 3. We define $\varepsilon_\pm = \varepsilon \pm \omega/2$, $\mathbf{p}_\pm = \mathbf{p} \pm \mathbf{q}/2$, and $z_\pm = |\mathbf{p}_\pm|^2/2m$. The noninteracting polarization function at finite μ is given by

$$\begin{aligned}\Pi(\mu,\omega,q) &= \mathrm{Tr}\, G(\mu,\varepsilon_+,\mathbf{p}_+)G(\mu,\varepsilon_-,\mathbf{p}_-) \\ &= \mathrm{Tr}\int \frac{d\varepsilon d^2p}{(2\pi)^3} \frac{1}{[i\varepsilon_+ - \mu - H_0(\mathbf{p}_+)][i\varepsilon_- - \mu - H_0(\mathbf{p}_-)]} \\ &= 2N\int \frac{d\varepsilon d^2p}{(2\pi)^3[\varepsilon_+ + i(\mu + z_+)][\varepsilon_+ + i(\mu - z_+)]} \\ &\quad \times \frac{(i\varepsilon_+ - \mu)(i\varepsilon_- - \mu) + z_+ z_- \cos 2\theta_{pq}}{[\varepsilon_- + i(\mu + z_-)][\varepsilon_- + i(\mu - z_-)]}, \end{aligned} \tag{61}$$

where θ_{pq} is the angle between $\mathbf{p}_+$ and $\mathbf{p}_-$. We now perform the integral over ε by residues to obtain

$$\begin{aligned}\Pi(\mu,\omega,\mathbf{q}) &= N\int \frac{d^2p}{(2\pi)^2} \frac{(z_+ + i\omega + z_- \cos 2\theta_{pq})\Theta(z_+ - \mu)}{z_+^2 - z_-^2 - \omega^2 + 2i\omega z_+} \\ &\quad + (\omega,\mathbf{q} \to -\omega,-\mathbf{q}) \\ &= N\int_{z_+=0}^{z_+=\mu} \frac{d^2p_+}{(2\pi)^2}\left[\frac{1}{z_+ + i\omega - z_-} - \frac{2z_- \sin^2\theta_{pq}}{(z_+ + i\omega)^2 - z_-^2}\right] \\ &\quad + (\omega,\mathbf{q} \to -\omega,-\mathbf{q}). \end{aligned} \tag{62}$$

In the limit $\mu \to 0$, this reproduces the noninteracting polarization function from Ref. 3. Now we expand Eq. (60) to leading order in small μ to obtain

$$\Delta F = -\frac{1}{2}\mu^2 \int \frac{d\omega d^2q}{(2\pi)^3} U(\omega,q) \frac{\partial^2\Pi(\mu,\omega,q)}{\partial\mu^2}. \tag{63}$$

The term linear in μ must vanish, by particle hole symmetry. Taking derivatives of Eq. (62) greatly simplifies the calculations since it turns the two-dimensional integral over momenta into a one dimensional integral over momentum angles, which is fully convergent, and may be evaluated numerically. We find

$$\frac{\partial^2\Pi}{\partial\mu^2} = N\frac{m}{2\pi}\frac{3\omega^2 z_q^2 - z_q^4}{(\omega^2 + z_q^2)^2}, \quad z_q = \frac{q^2}{2m}, \tag{64}$$

$$\Delta F = -\frac{\mu^2}{2}\int \frac{d\omega d^2q}{(2\pi)^3} U(\omega,\mathbf{q}) \frac{\partial^2\Pi}{\partial\mu^2}. \tag{65}$$

We again change to the coordinates $\omega = r\cos\theta$, $z_q = r\sin\theta$, and measure r in units of E_0. Note that even though the interaction has a pole at $\theta \to 0, \pi$, this pole is canceled by $\partial^2\Pi/\partial\mu^2$ having a zero at $\theta \to 0, \pi$. As a result, the θ integral is fully convergent. Integrating numerically over θ and analytically over r, we find that the fractional change in the compressibility is

$$\frac{\delta K(\xi)}{K(0)} = \frac{0.56}{2N\pi \ln 4}\xi \tag{66}$$

a result that agrees exactly with Eq. (57). We note that an enhancement of the compressibility due to interactions was also predicted in Ref. 23. However, the effect described by Eq. (57) is much weaker than that predicted in Ref. 23 because we have worked with a screened interaction whereas in Ref. 23 screening was not taken into account.

In summary, the compressibility does not renormalize at leading (log square) order, just as in the Luttinger liquids and while there is a subleading logarithmic correction, the prefactor is quite small $[0.56/(2N\pi \ln 4) \approx 0.016]$. Thus, in contrast to the zero-bias anomaly in TDOS, experimental detection of the interaction correction to the compressibility is likely to be challenging. The difference arises because the single log flows are much weaker than the $\log^2$ flows, retrospectively justifying our earlier neglect of the single log flows in the RG. Hence, strong suppression of the tunneling density of states at energy scales where the compressibility is not significantly renormalized is a key signature of the marginal Fermi liquid physics in bilayer graphene.

X. DISCUSSION AND CONCLUSIONS

Here we briefly discuss the range of validity of our results. Our analysis was organized as a perturbation theory in $\Gamma^2 Z^2/N$. Since $\Gamma Z = 1$ at leading (log square) order, the perturbation theory remains well defined under the log square flows. However, our analysis neglected subleading single log flows. For $\xi \approx N\pi^2$, the subleading single log flows become important, and the analysis leading to the expression Eq. (44) no longer applies. A mean field theory of subleading single log effects[3] indicates that a gapped state develops at $\xi = \frac{3}{13}N\pi^2$, the scale which we tentatively identify as the limit of validity of our analysis.

How can the marginal Fermi liquid physics be distinguished from the formation of a gapped state? We note that at very low energies, once the gapped state has developed, both the tunneling density of states and the compressibility will vanish. What we have shown, however, is that there is a large range of energies greater than the energy scale for gap formation, where the tunneling density of states vanishes while the compressibility remains essentially unchanged. Such behavior represents the key signature of the marginal Fermi liquid physics discussed above, which is analogous to the Luttinger liquid physics.

In our analysis, we neglected the short range interactions which are characterized by lattice scale, such as the interlayer density difference interaction $V_- = \frac{1}{2}(V_{AA} - V_{AB}) = \pi e^2 d$ and the Hubbard-type on-site repulsion. Short range interactions are nondispersive, do not renormalize the Green's function in the weak coupling limit, and hence do not alter our results. Short range interactions also produce only single log renormalization[4,5] and therefore do not need to be included in our log square RG. Similarly, we justify our neglect of the

trigonal warping effect[24] by noting that trigonal warping is significant only on energy scales smaller than the characteristic energy scale for onset of gapped states.[3]

Finally, we note that our analysis made use of the fact that there were no uncanceled log square divergences at one loop order in the RG, except for the renormalization of the quasiparticle residue and the Coulomb vertex function, which were related by a Ward identity, Eq. (29). Technically, in order for our neglect of higher loop corrections to be justified, we also require that there are no uncanceled log square divergences beyond one loop order in the RG, except those that are constrained by Ward identities. We believe this to be the case, however, the proof requires a nonperturbative approach, which lies beyond the scope of the present work.

To conclude, we have examined the one-loop RG flow for bilayer graphene. We have demonstrated that the quasiparticle residue Z and the Coulomb vertex function Γ both flow as ξ^2, where ξ is the RG time. All other quantities flow only as ξ. The structure of the RG for Coulomb interacting BLG has strong similarities to the RG for the one dimensional Luttinger liquids. In particular, we predict a strong interaction suppression of the tunneling density of states for undoped BLG, even at energy scales where the electronic compressibility is essentially unchanged from its noninteracting value. These predictions may be readily tested by experiments.

ACKNOWLEDGMENTS

We acknowledge useful conversations with A. Potter and P. A. Lee. This work was supported by Office of Naval Research under Grant No. N00014-09-1-0724.

[1] K. S. Novoselov, E. McCann, S. V. Morozov, V. I. Fal'ko, M. I. Katsnelson, U. Zeitler, D. Jiang, F. Schedin, and A. K. Geim, Nat. Phys. **2**, 177 (2006).
[2] H. Min, G. Borghi, M. Polini and A. H. MacDonald, Phys. Rev. B **77**, 041407(R) (2008).
[3] R. Nandkishore and L. Levitov, Phys. Rev. Lett. **104**, 156803 (2010).
[4] F. Zhang, H. Min, M. Polini, and A. H. MacDonald, Phys. Rev. B **81**, 041402(R) (2010).
[5] O. Vafek and K. Yang, Phys. Rev. B **81**, 041401(R) (2010).
[6] K. Sun, H. Yao, E. Fradkin, and S. A. Kivelson, Phys. Rev. Lett. **103**, 046811 (2009).
[7] Y. Barlas and K. Yang, Phys. Rev. B **80**, 161408(R) (2009).
[8] I. E. Dzyaloshinskii and A. I. Larkin, Zh. Eksp. Teor. Fiz. **65**, 411 (1973) [JETP **38**, 202 (1974)].
[9] R. Shankar, Rev. Mod. Phys. **66**, 129 (1994).
[10] T. Giamarchi, *Quantum Physics in One Dimension* (Clarendon, Oxford,2005).
[11] B. L. Altshuler, A. G. Aronov, and P. A. Lee, Phys. Rev. Lett. **44**, 1288 (1980).
[12] A. M. Finkelstein, Zh. Eksp. Teor. Fiz. **84**, 168 (1983) [Sov. Phys. JETP **57**, 97 (1983)].
[13] R. Nandkishore and L. Levitov, Phys. Rev. B (to be published), arXiv:1009.0497 (unpublished).
[14] We have performed a unitary transformation on the Hamiltonian, as outlined in Ref. 13, to clearly manifest the symmetries. As a consequence, our "valley" and "sublattice" variables are not the physical valley and sublattice variables but are linear combinations thereof.
[15] E. McCann, Phys. Rev. B **74**, 161403(R) (2006).
[16] J. Nilsson, A. H. Castro Neto, N. M. R. Peres, and F. Guinea, Phys. Rev. B **73**, 214418 (2006).
[17] The symmetry of the Hamiltonian may be spontaneously broken. However, the energy scale for spontaneous symmetry breaking is set by the subleading single log flows (Ref. 3) and is lower than the energy scale for the phenomena discussed in this paper.
[18] In that, we ignore vertices of the form $Y_{AAAB}\partial_+^2$, $Y_{AABA}\partial_-^2$, and other similar terms, which are allowed by symmetries but are irrelevant in the RG sense.
[19] J. Gonzalez, F. Guinea and M. A. H. Vozmediano, Phys. Rev. B **59**, R2474 (1999).
[20] V. B. Berestetskii, E. M. Lifshitz, and L. P. Pitaevskii, *Quantum Electrodynamics*, Landau and Lifshitz, Course of Theoretical Physics Vol. 4 (Butterworth-Heinemann, Oxford, 1979), Chap. 11.
[21] Yu. V. Nazarov, Zh. Eksp. Teor. Fiz. **96**, 975 (1989) [Sov. Phys. JETP **68**, 561 (1989)].
[22] L. S. Levitov and A. V. Shytov, Pis'ma Zh. Eksp. Teor. Fiz. **66**, 200 (1997) [JETP Lett. **66**, 214 (1997)].
[23] S. V. Kusminskiy, J. Nilsson, D. K. Campbell, and A. H. Castro Neto, Phys. Rev. Lett. **100**, 106805 (2008).
[24] E. McCann and V. I. Falko, Phys. Rev. Lett. **96**, 086805 (2006).